Talanta 246 (2022) 123496

Contents lists available at ScienceDirect

Talanta

journal homepage: www.elsevier.com/locate/talanta

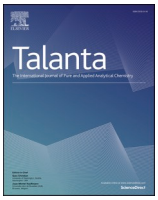

Biotin-streptavidin sandwich integrated PDA-ZnO@Au nanocomposite based SPR sensor for hIgG detection

Haohua Yang, Xueqi Zhao, Ziwei Zhang, Pinyi Ma, Xinghua Wang, Daqian Song, Ying Sun *

College of Chemistry, Jilin Province Research Center for Engineering and Technology of Spectral Analytical Instruments, Jilin University, Qianjin Street 2699, Changchun, 130012, China

ARTICLE INFO

Keywords:
PDA-ZnO@Au nanocomposite
hIgG detection
SPR based Sensor
Streptavidin-biotin

ABSTRACT

SPR is a mature optical biosensor technology for detecting biomolecular interactions without fluorescence or enzyme labeling. In this paper, we acquire a sensitive SPR biosensor based on ZnO@Au nanomaterial, and the classical sandwich strategy using biotin-streptavidin for secondary signal amplification system was used to detect human IgG (hIgG). Nano-zinc oxide (ZnO) has the dual characteristics of nanocomposite and traditional zinc oxide, with large specific surface area and high chemical activity. Besides, the gold-coated ZnO nanocrystals improve the optical properties of ZnO and enlarge the loading capacity with better biocompatibility. Therefore, a sensing platform based on PDA-ZnO@Au nanomaterial was constructed on gold film modified with mercaptan. Meanwhile, the biotin-avidin system in SPR sensor field has been rapidly developed and applied. Due to the highly selection of streptavidin (SA) and biotin interact with each other, GNRs-SA-biotin-Ab_2 (GSAB-Ab_2) were constructed to obtain the secondary enhancement of SPR signal. The influences of experimental conditions were also discussed. With optimal experimental conditions, introducing GSAB-Ab_2 conjugate combined with a sandwich format, the resulting SPR biosensor provides a favourable range for hIgG determination of 0.0375–40 μg mL^{-1}. The minimum detection concentration of hIgG that can be obtained by this method is approximately 67-fold lower than the conventional SPR sensor based on gold film. The sensitivity of SPR biosensor is significantly improved in a certain range.

1. Introduction

Nanohybrid materials have always played an important role in surface plasmon resonance sensing technology [1]. Nanohybrid materials have many general categories such as noble metal nanoparticles, magnetic nanoparticles, zinc oxide, molybdenum disulfide, graphene and multi-walled carbon nanotubes [2]. These nanohybrid materials have good biocompatibility [3], catalysis [4]and adsorption [5], which could catalyse, conduct electrons and amplify response signals. The sensing film of the conventional SPR sensor is pure thin metal film, which leads to its low specific surface area, low load and weak sensitivity [6]. Thus, the introduction of nanohybrid materials can produce electromagnetic coupling effect with the gold film of SPR sensor so as to amplify SPR response signal and improve detection sensitivity significantly. Nano-zinc oxide has large specific surface area and high chemical activity, but it is arduous to stably exist in aqueous solution [7]. Generally, metal nanoparticles are coated on the surface of nano-zinc oxide particles to modify their surface so that they can be uniformly dispersed into the aqueous solution for biological detection [8,9]. In this paper, we synthesized ZnO@Au nanocomposite particles. ZnO nanocrystals were used as seed crystals and Au was gradually deposited on the surface to form ZnO@Au nanocomposite particles. ZnO@Au nanocomposite particles are immobilized to the SPR sensor chip by molecular self-assembly to increase the response signal of SPR biosensor.

Biotin act as a coenzyme for carboxylase enzymes with a molar mass of 66 kDa and is found in small amounts in tissues and blood [10]. Avidin is a tetrameric protein with an approximate molar mass of 60 kDa [11]. In the field of immunoassay, not much different from avidin is SA, but the SA produced by Streptomyces is also tetrameric protein (not glycosylated) with stronger inertness and weaker non-specific binding [12], resulting in better specific binding and higher sensitivity. The interaction between biotin and SA has a very high affinity independent of the covalent bond between molecules, and the affinity constant is 1015 L mol^{-1} [13], which is one of the strongest reported affinity systems, about dozens or hundreds of times compared to the antigen (Ag)-antibody interaction [14]. The biotin-SA system can be used as a

* Corresponding author.
E-mail address: yingsun@jlu.edu.cn (Y. Sun).

https://doi.org/10.1016/j.talanta.2022.123496
Received 29 December 2021; Received in revised form 9 April 2022; Accepted 19 April 2022
Available online 21 April 2022

molecular connector for the connection between antibody and signal molecules due to the excellent binding strength and speed [15]. The antibody binds to the biotin in a mild way that does not reduce the bioactivity of the antibody, and then a signal molecule functionalized by SA is added [16]. The synthesized GNRs-SA-biotin-Ab_2 composite material can accommodate more signaling molecules, and the larger molecular weight increase the refractive index, thus greatly improving the SPR signal strength.

HIgG is the main antibody component in human serum [17]. HIgG levels in humans are commonly associated with diseases such as humoral immune diseases [18], infectious diseases [19], liver diseases [20] and rheumatoid arthritis [21]. Therefore, detection of hIgG is of great significance for early diagnosis of related diseases. Many analytical methods have been used to detect hIgG in human serum, such as chemical luminescence analysis [22], fluorescence analysis [23] and enzyme-linked immunosorbent assay [24]. Compared to the above methods, SPR technique measures the refractive index change in response to the interaction of biomolecules on the gold film and is suitable for hIgG detection due to its advantages of no labeling, no purification and real-time detection [25,26].

In this work, a self-assemble SPR biosensor was embellished using ZnO@Au nanocomposite particles as the support platform to attain the rapid detection of hIgG. The ZnO@Au were modified on the gold film surface, forming a sensing interface. With the increase of hIgG concentration, the wavelength shift value of SPR gradually increase. Further, to improve the sensitivity detection of hIgG, GSAB-Ab_2 was introduced to realize the secondary amplification of SPR signal. Combining with the above complex, a novel sandwich-type SPR biosensor was fabricated (Fig. 1). The resulting ZnO@Au based biosensor with GSAB-Ab_2 used as the signal molecules of secondary amplification shows ultrasensitive response to hIgG with good selectivity, good reproducibility and high recoveries in human serum samples.

2. Materials and methods

2.1. Materials

Biotinamidohexanoyl-6-aminohexanoic acid N-hydroxysuccinimide ester (biotin-XX-NHS), N-hydroxysuccinimide (NHS), 3-mercaptopropionic acid (MPA) and bovine serum albumin (BSA) were purchased from Aladdin Industrial Corporation. Streptavidin (SA) was purchased from Shanghai Macklin Biochemical Co., Ltd. Zinc nitrate hexahydrate ($Zn(NO_3)_2{\cdot}6H_2O$) was purchased from Xilong Chemical Co., Ltd. Sodium hydroxide (NaOH) was purchased from Beijing Chemical Works. 1,6-hexanedithiol (HDT) was purchased from Jkchemical. 1-ethyl-3-(3-dimethylaminopropyl)carbodiimide (EDC), Hydrogen tetrachloroaurate hydrate ($HAuCl_4{\cdot}3H_2O$) and Dopamine hydrochloride (DA) were purchased from Saen Chemical Technology (Shanghai) Co., Ltd. Sodium borohydride ($NaBH_4$), Hexadecyl trimethyl ammonium Bromide (CTAB) and ascorbic acid (AA) were purchased from Sinopharm Chemical Reagent Co. Ltd. Silver nitrate was purchased from Thermo Fisher Scientific Co., Ltd. Rabbit anti-hIgG, hIgG, rabbit IgG and bovine IgG were purchased from Beijing Biosynthesis Biotechnology Company and were stored at −20 °C. Chicken serum sample were obtained from the Life Sciences College of Jilin University (Changchun, China). All animal experiments were conducted in accordance with the guidelines of the Regional Ethics Committee for Animal Experiments established by the Jilin University Institutional Animal Care and Use. 0.01 mol L^{-1} sodium phosphate buffered saline (PBS, pH 7.4) and 10 mmol L^{-1} tris-buffer (pH 8.5) were freshly prepared.

All deionized (DI) water used in the experiment was prepared by a Millipore purification device. Rabbit anti-hIgG, hIgG, mouse IgG and bovine IgG were preserved at −20 °C and some reagents were preserved at 4 °C.

2.2. Instruments

UV–Vis were recorded using a Cary-60 spectrometer (Agilent Technologies Inc., USA). All pH measurements were taken with a PHS-3C pH-Meter (INESA Scientific Inc., China). Transmission electron microscopy (TEM) images of GNRs, GNRs-SA, AuNPs and ZnO@Au were obtained using a H-8100 transmission electron microscope (TEM, Hitachi High-Tech Co., Japan) operating at 200 kV. The main equipment used in this experiment is the wavelength - modulation SPR sensor assembled by our research group. A 50 nm gold layer was deposited on the surface of K9 glass cover glass. Cedar oil with the same refractive index as K9 glass is used to adhere on the surface of prism made of K9 glass. With the iodine tungsten lamp as the light source, the white light emitted by the light source passes through the lens and the polarized plate to form parallel polarized light, and then enters the optical prism system of the SPR. Firstly, the parallel polarized light is irradiated on the side surface of the prism, and then refracted to the bottom of the prism to excite the surface plasmon at the interface between the coating metal and the sample solution. The light that goes through total internal reflection is refracted out by the other side of the prism and focused into the micro fiber optic spectrometer (HR2000+, Ocean Inc., USA).

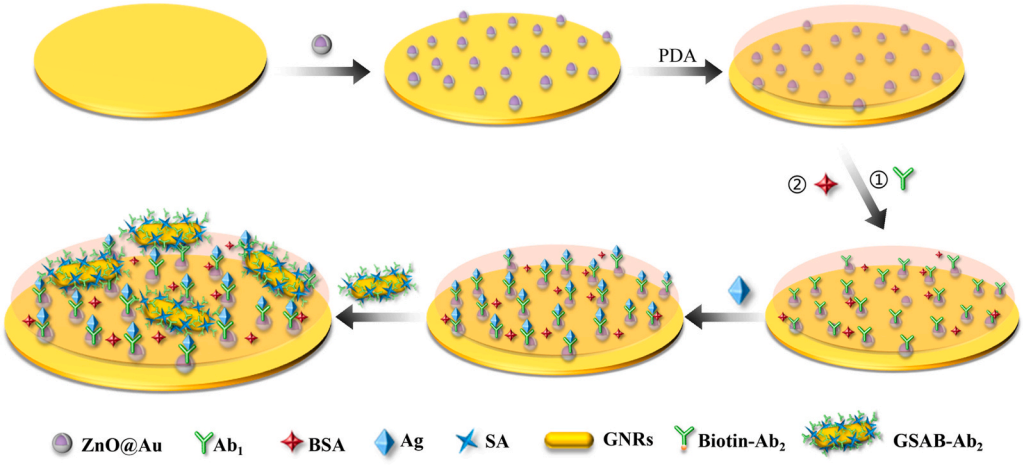

Fig. 1. A schematic diagram of experimental procedure.

2.3. Procedures

2.3.1. Synthesis of gold nanorods (GNRs)

The seed growth method was used to synthesize GNRs [27]. First, the seed solution was prepared: The frozen 0.6 mL $NaBH_4$ (0.01 mol L^{-1}) solution was added to a mixture of 5 mL $HAuCl_4$ (0.5 mmol L^{-1}) and 5 mL CTAB (0.2 mol L^{-1}). The mixture was stirred strongly for 2 min and then stood at 25 °C for 2 h to obtain a tawny solution. The second step was to prepare growth solutions: 50 mL CTAB (0.2 mol L^{-1}) solution, 50 mL $HAuCl_4$ (1 mmol L^{-1}) solution and 3 mL $AgNO_3$ (0.004 mol L^{-1}) solution was mixed at room temperature, and then 0.7 mL of 0.1 mol L^{-1} AA was added. The solution changed from dark yellow to colorless. Finally, 0.24 mL of seed solution was added to the growth solution, which was incubated at 28 °C for 24 h, washed for three times by high-speed centrifugation (rotating speed 14,000 rpm), and re-dispersed in deionized water to obtain fully grown GNRs solution.

2.3.2. Streptavidin functionalization of GNRs

Briefly, 130 μL of aqueous solutions of streptavidin (50 μg μL^{-1}) were added 1 mL of colloidal solutions of AuNPs [28]. The mixtures were gentle oscillated at room temperature for overnight. The mixtures were centrifuged to remove the excess streptavidin. Finally, SA-functionalized GNRs (SA-GNRs) were obtained the mixtures and then restored in deionized (DI) water.

2.3.3. Preparation of Ab_2-biotin-XX-NHS and ZnO@Au

50 μL of rabbit anti-human lgG antibody (50 μg μL^{-1}) were mixed with 2 μL of biotin-XX-NHS (i.e. NHS-activated biotin with a 14 atom spacer arm) which was dissolved in DMSO at 1 mg mL^{-1} [29]. The mixture was incubated at room temperature with gentle shaking for 3 h. The resulting mixture was referred to as Ab_2-biotin solution and stored at 4 °C.

4 mL ethanol solution of $Zn(NO_3)_2{\cdot}6H_2O$ (0.05 mol L^{-1}) was mixed with 3–4 mL of the above prepared AuNPs, and 4 mL ethanol solution of sodium hydroxide (0.25 mol L^{-1}) was added to stir vigorously for 1 h to obtain white purple precipitation under the action of coprecipitation [30]. Finally, the ZnO@Au is obtained by centrifugation (8000 rpm, 20 min).

2.3.4. Modification of sensing platform

The Au film layer was immersed into a 10 mmol L^{-1} HDT solution for 24 h. Then, the Au film was rinsed repeatedly with ethanol and deionized water, followed by drying under N_2. The modified film was immersed into the ZnO@Au solution for 12 h. Then, the HDT- ZnO@Au modified Au film was removed from the solution and washed with ethanol and ultrapure water, followed by drying under N_2. Next, the ZnO@Au -HDT Au film was immersed into a 0.5 mg mL^{-1} PDA solution for 0.5 h, then washed with ultrapure water and dried under gaseous N_2.

2.3.5. Antibody immobilization

The PDA-ZnO@Au modified gold film is installed at the bottom of the reactor to form a flow cell. PBS was injected into the flow cell as baseline solution. When the resonant wavelength was maintained constant, 100 μg mL^{-1} rabbit anti-hIgG (Ab_1) was directly injected into flow cell. The unbound antibodies were removed by PBS injection, 10 mg mL^{-1} BSA solution was injected to seal the non-specific binding sites on the surface of the sensing membrane.

2.3.6. Immunoassay

After attaching the Ab_1 to the surface of the sensing membrane, a sequence of different concentrations hIgG diluted with PBS was separately injected into the flow cell. After 1 h, the specific binding of Ab_1 and hIgG was completed. PBS was injected to remove the unbound hIgG. After the resonant wavelength was stable, the prepared 500 μL of 500 μg mL^{-1} GSAB-Ab_2 was injected in the flow cell for 50 min to form a sandwich structure (Ab_1/Ag/GNRs-SA-biotin-Ab_2) on the sensor substrate. Finally, PBS was used to remove unbound GSAB-Ab_2 in the reactor. The SPR sensor responses were determined as the shifts of resonant wavelength before sample injection and after rinsing with PBS. All experiments were conducted in triplicate.

3. Results and discussion

3.1. Characterization

The morphology and size of the prepared GNRs, GNRs-SA, AuNPs and ZnO@Au were investigated by transmission electron microscopy (TEM). According to the normal distribution curve, the as-prepared GNRs have average diameter and length of 13 ± 3 nm and 47 ± 3 nm, respectively (Fig. S1 and Fig. S2). TEM of GNRs synthesized by CTAB seed-mediated method is shown in Fig. 2a. The seed liquid is usually nanocrystalline isotropic growth nuclei, and the yellow Au^{3+} in the growth liquid is reduced to colorless Au^{+} under the action of weak reducing agent ascorbic acid. During seed growth, the Ag surface coverage was higher at the beginning of the reaction. Ag^{+} in $AgNO_3$ and Br^{-} in CTAB will form silver bromide solid, leading to the reduction of charge density of Br^{-} and repulsion between CTAB head group, which is conducive to the formation of long rod template. Besides, when gold interacts with CTAB, silver bromide deposits on the {110} surface of GNR and promotes the growth of GNR on other specific crystal planes. Meanwhile, Ag^{+} was reduced by ascorbic acid to form pentagonal Ag twin nanostructures. CTAB surfactants are preferentially connected to the surface of Ag twin nanostructures [31]. With the passage of time, the deposition rate of Ag slowed down and Ag diffused into the GNRs. By the first 45 min of the reaction, the Ag surface coverage was close to zero until the end of the reaction. Finally, Ag reduces Au^{+} to Au^{0} to obtain unidirectional growth. And the aspect ratio is about 3.62 with calculation. After the introduction of SA, the two are assembled to form nanocomplexes GNRs-SA under the action of electrostatic force. As shown in Fig. 2b, the modification of SA enables the edge of GNRs to become obscure, indicating the triumphant modification of the SA on the transverse terminal of the GNRs. TEM of AuNPs and ZnO@Au nanocomposite particles are exhibited in Fig. 2c and d, respectively.

UV–vis absorption spectra of the GNRs, GNRs-SA, and ZnO@Au synthesized in this task are illustrated in Fig. 3a. GNRs has two ultraviolet absorption peaks, which are transverse absorption peak at 520 nm and longitudinal absorption peak at 754 nm. The longitudinal absorption peak of GNRs-SA was red-shifted about 21 nm compared to the GNRs, which was induced by the change of the refractive index near the GNRs surface. As shown in Fig. 3b, the UV–vis absorption peaks of AuNPs and ZnO@Au nanomaterials are located at 530 nm and 520 nm. UV–vis absorption spectra of the Ab_2 and Ab_2-biotin are illustrated in Fig. 3c, with peaks 280 nm and 265 nm, respectively.

3.2. Immobilization of rabbit anti-hIgG

Dopamine (DA), a crucial neurotransmitter, can self-polymerize under very mild response conditions [32]. In a slightly alkaline solution with oxygen as an oxidant, dopamine monomers spontaneously polymerize to form polydopamine (PDA), which has strong adhesion to the substrate surface [33]. PDA coating can increase the hydrophilicity, biocompatibility and chemical stability of nanomaterials. PDA can be used as a reducing agent to reduce Au^{+}, Ag^{+}, Pt^{+} and other precious metal ions in alkaline environment [34]. In the process of PDA formation, two electrons were released when DA was oxidized to DA-quinone, which reduced the metal salts to their corresponding metals and produced metal nanoparticles that deposited on the surface of the PDA [35]. Besides, the PDA could directly immobilize the antibody without further processing due to Schiff base reaction between the two [36]. PDA-ZnO@Au modified SPR sensor chip based on the self-polymerization of dopamine and the in-situ reduction ability of gold ions was used to detect hIgG in this work.

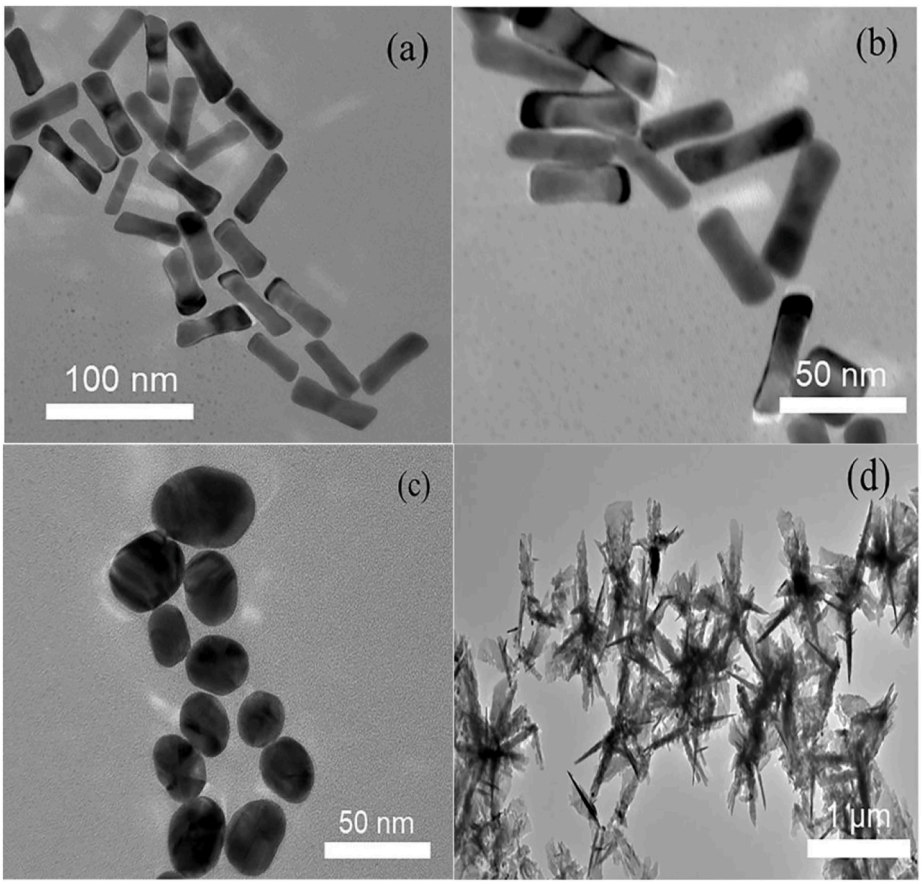

Fig. 2. TEM images of (a) GNRs, (b) GNRs-SA, (c) AuNPs, and (d) ZnO@Au.

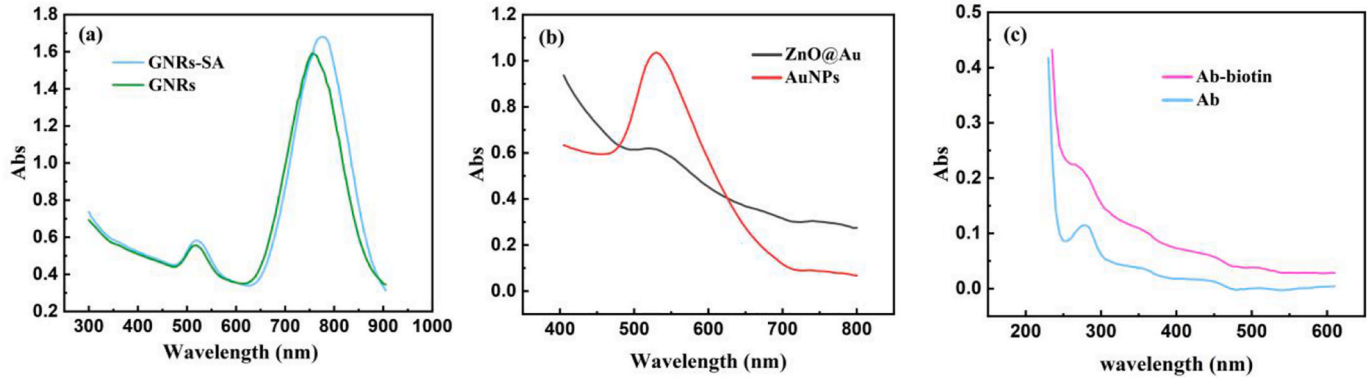

Fig. 3. UV–vis absorption pectrum of (a) GNRs-SA and GNRs, (b) ZnO@Au and AuNPs, (c) Ab-biotin and Ab.

Different amounts of antibodies were injected into the flow cell and the concentrations of antibodies were optimized by monitoring the changes of SPR wavelength (Δλ). The resonant wavelengths were differently red-shifted with the increase of the concentration of Ab_1. To achieve optimal experimental parameters and good analytical performance of the SPR biosensor, we optimized the immobilized concentration and reaction time of Ab_1. Different concentrations of Ab_1 were injected into the flow cell. Fig. 4a shows the dynamic adsorption curve of fixed Ab_1, redshift of the resonant wavelength was observed with the reaction time. After 80 min, the resonance wavelength remained basically unchanged, indicating that the Ab_1 fixed on the surface of the biosensor approached saturation, and 80 min was selected as the optimal Ab_1 immobilization time. At concentration of 100 μg mL^{-1}, the maximum wavelength shifts were observed. We increased the antibody concentration to 125 μg mL^{-1} and found no significant shift in wavelength compared to the concentration of 100 μg mL^{-1}, indicating that Ab_1 attached on PDA-ZnO@Au had reached saturation. Therefore, 100 μg mL^{-1} was selected as the optimal concentration for antibody fixation in this experiment and the maximum resonance wavelength shift within 80 min was 10.5 nm.

3.3. Optimum binding amount of GNRs-SA

Coomassie bright blue method [37] was used to quantitatively analyze the optimal binding amount of SA on GNRs. In a nutshell, different amounts of SA were added into 1 mL of GNRs, so that the concentrations of SA were 45 μg mL^{-1}, 55 μg mL^{-1}, 65 μg mL^{-1}, 75 μg mL^{-1}, 85 μg mL^{-1}, 95 μg mL^{-1}, 110 μg mL^{-1}, 130 μg mL^{-1} and 150 μg

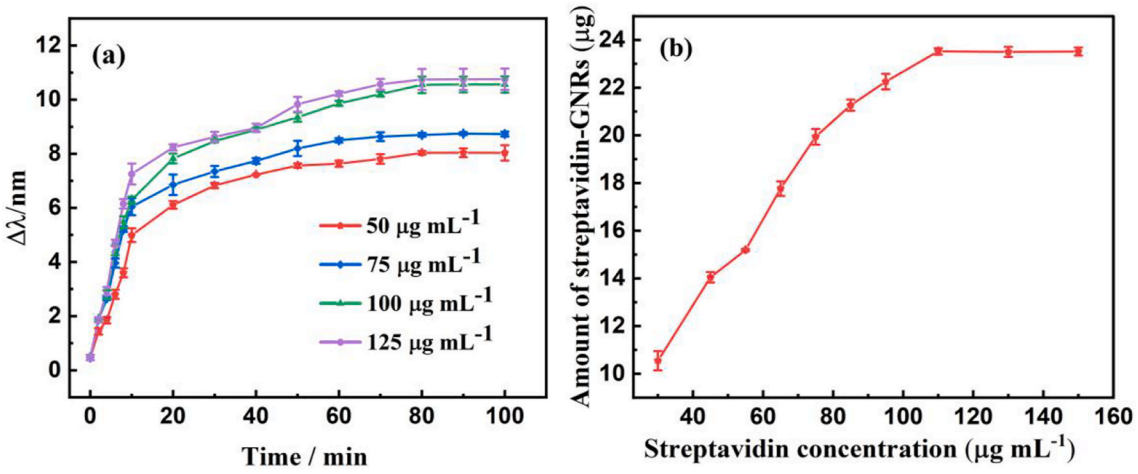

Fig. 4. Kinetic adsorption curves of gradient concentrations of rabbit anti-human antibody on PDA-ZnO@Au-based sensing platform (a), and effect of streptavidin concentration on amount of streptavidin attached to GNRs (b).

mL^{-1}, respectively. The reaction was oscillated overnight, and the free SA in the supernatant was obtained by centrifugation. The reaction ratio of Coomassie Brilliant Blue and the supernatant was 5:1 (v/v). The absorbance at 595 nm was recorded with a UV–Vis spectrophotometer, and the amount of SA bound on GNRs was calculated by the absorbance. As seen from the Fig. 4b, the binding amount of the two increased continuously with the increasing amount of SA, and reached the maximum when the reaction concentration of SA reached 110 μg mL^{-1} and remained unchanged with the increasing concentration of SA, indicating that the binding amount of the two reached saturation. Therefore, 110 μg mL^{-1} of SA was determined as the optimal reaction concentration for the combination of GNRs-SA.

3.4. Secondary signal amplifier-enhanced immunoassay

For SPR sensing film, large surface area, high chemical activity and high loading capacity are the most effective way to conjugate more antibodies based on ZnO@Au sensing substrates and enhance SPR biosensor sensitivity. For biotin and SA systems, each antibody can connect multiple biotin small molecules, and each SA has four biotin binding sites, which makes the complex of GSAB-Ab_2 accommodate more signal molecules, thus amplifying the terminal signal. To further elevate the sensitivity for detecting hIgG, the classical sandwich strategy was applied. Compared to AuNPs with only one plasma absorption band, GNRs have two plasma absorption bands due to different transverse and longitudinal surface charge densities, which are located at 520 nm on the short axis and tunable near infrared band on the long axis respectively [38]. The longitudinal plasma absorption band is very sensitive to the change of refractive index of the surrounding medium, which increases the sensitivity. The longitudinal absorption peak of GNRs varies continuously from visible to near infrared region with different aspect ratio [39]. In addition, GNRs have a larger specific surface area, which can fix more biomolecules and amplify the response signal, further improving the sensitivity. GNRs-SA-biotin composites decorated with Ab_2 as signal enhancers were employed into the sensing system to combine with hIgG captured on the surface of the sensing chip. The collective oscillation and local surface plasmon resonance of conducting electrons in the GNRs enhance the local electric field near GSAB-Ab_2 composites. Meanwhile, the interaction between the local surface plasma of GNRs and the plasma on the surface of ZnO@Au-based gold film amplifies the SPR response signal. Besides, the GSAB-Ab_2 composites markedly enlarge the thickness of the sensing chip and increase the refractive index of the sensing chip thereby amplifying the response signal. As the amount of GSAB-Ab_2 composites is linked to sensitivity enhancement, we optimized the amount of GSAB-Ab_2 composites to be used in final assay. The resonant wavelength displayed increasing redshifts with the injection of increasing amounts of GSAB-Ab_2 composites up to a final concentration of 500 μg mL^{-1}, and saturation had been

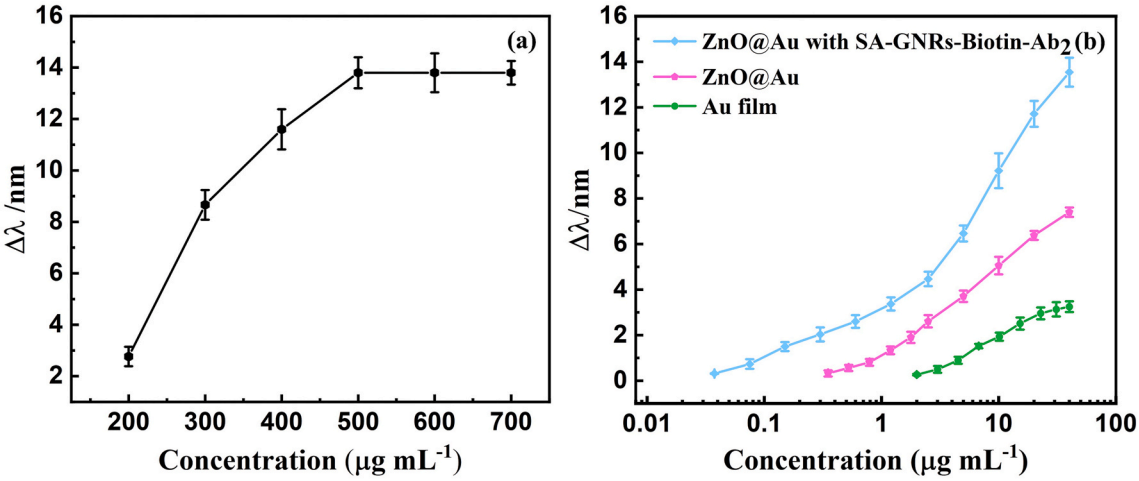

Fig. 5. Optimization of concentrations of GSAB-Ab_2 solutions (a), and relationships between concentrations of hIgG and the resulting resonant wavelength shifts in the three detection formats: biosensor based on ZnO@Au with the GSAB-Ab_2 sandwich assay; biosensor based on ZnO@Au and biosensor based on Au film (b).

reached (Fig. 5a). This result indicates that 500 μg mL^{-1} is the optimal concentration of GSAB-Ab_2 composites.

Next, the SPR biosensor was designed to test its performance by detecting different concentrations of hIgG. Fig. 5b shows the relationship between the shift of resonance wavelength and the change of hIgG concentration in SPR sensors with different assay (biosensor based on ZnO@Au with the GSAB-Ab_2 sandwich assay; biosensor based on ZnO@Au and biosensor based on Au film). The ZnO@Au-based SPR biosensor with the GSAB-Ab_2 sandwich assay exhibited the best response to hIgG at concentrations ranging from 0.0375 to 40.00 μg mL^{-1}, and the maximum resonance wavelength shift is 13.54 nm. The ZnO@Au-based SPR biosensor exhibited a good response to hIgG at concentrations ranging from 0.35 to 40.00 μg mL^{-1}, and the maximum resonance wavelength shift is 7.40 nm. The SPR biosensor based on gold film exhibited a response to hIgG at concentrations ranging from 2.50 to 40.00 μg mL^{-1}, and the maximum resonant wavelength shift was 3.25 nm. As can be seen from the above data, the detection limit determined by the present method based on the ZnO@Au substrate with the GSAB-Ab_2 sandwich assay was about 67-fold and 9-fold lower than that of ZnO@Au-based and Au film-based sensing platform respectively, which evidently enhanced the sensitivity of the SPR biosensor. Comparison of performance for the detection of IgG obtained by those reported in the literature and current work by SPR sensor are listed in Table 1.

3.5. Specificity of the assay

The specificity of the designed SPR biosensor was examined by testing rabbit IgG, bovine IgG and hIgG. After the immobilization of the rabbit anti-hIgG on the biosensor surface, rabbit IgG, bovine IgG and hIgG at a concentration of 10 μg mL^{-1} were separately injected into the flow cell. The results indicated that other antigens exhibit no response SPR signals compared to hIgG (Fig. 6). Furthermore, the present SPR biosensor offers high specificity toward hIgG. The prepared sensing chip can be reused by impulse injection of massive PBS into the flow cell to dissociate antigen from antibody immobilized on the sensing platform. As showed in Fig. S3, the prepared biosensor exhibits about 76% of the initial activities after reusing for the fourth time, which indicated the sensor had good reusability in 7 days.

3.6. Recoveries of method in serum

Selectivity and sensitivity are important performance parameters of biosensors especially for analyzing complex samples. The application of the biosensor in real samples was verified by the spiked recovery experiment. Adding different concentrations of hIgG (2.5, 5 and 10 μg mL^{-1}) to blank chicken serum samples. In addition, PBS samples containing the same standard level were used as controlled experiment. The recovery of the experiment was defined as the ratio of resonant wavelength shifts from injecting chicken serum and PBS containing the same spiked level of hIgG ($\Delta\lambda_{serum}/\Delta\lambda_{PBS}$). As reported in Table 2, the resulting recoveries were 105.0–117.8%, suggesting that the accuracy and reproducibility of GSAB-Ab_2 based immunoprobe and ZnO@Au SPR biosensor are acceptable.

4. Conclusion

In summary, an original SPR sensing platform based on ZnO@Au nanomaterial, and the classical sandwich strategy using biotin-streptavidin for secondary signal amplification system was used to detect hIgG. The prepared ZnO@Au based on sensing platform is convenient to be prepared, enlarge the loading capacity and has good biocompatibility. The introduction of GSAB-Ab_2 signal enhancers provides noteworthy sensitivity enhancement through abundant enrichment of hIgG, fast mass transfer and increase the refractive index. The result with low detection limit of hIgG achieved by the proposed sensing platform has been lowered to 0.0375 μg mL^{-1}, which is approximately 67-fold lower and 9-fold lower than the ZnO@Au-based sensing platform and the conventional SPR sensor based on gold film, respectively. The obtained recoveries of spiked human serum samples suggest good selectivity and sensitivity in practical applications. The strategy presented for detecting hIgG can be easily expanded to the clinical determination of other diagnostic markers which have available corresponding epitopes.

Table 1
Comparison of performance obtained by current work and those reported in the literature.

Method	Detection limit	Reference
cGO/SNCs-antigen conjugate-based biosensor	0.075 μg mL^{-1}	[40]
AIgG anchored 5CB LC microdroplets assay	0.016 μg mL^{-1}	[41]
PDA-Au conjugate-based optical fiber biosensor	2.00 μg mL^{-1}	[42]
OFET based on biosensor	0.62 μg mL^{-1}	[43]
rGO-based SPR assay	0.15 μg mL^{-1}	[44]
ZnO@Au based GSAB-Ab_2 sandwich assay	0.0375 μg mL^{-1}	This work

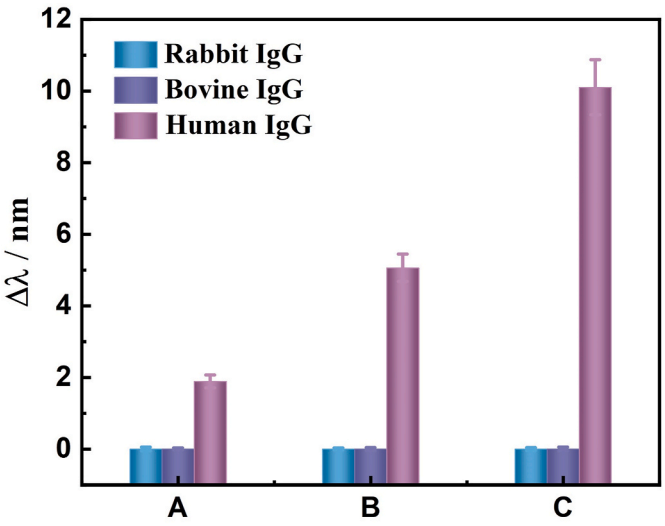

Fig. 6. The shifts of the resonant wavelength measured with different antigens (rabbit IgG, bovine IgG and hIgG) in different assays: (A) Au film; (B) ZnO@Au and (C) ZnO@Au with the GSAB-Ab_2 sandwich assay.

Table 2
Analytical results of hIgG in human serum (n = 3).

Content of HIgG (μg mL^{-1})	Spiked (μg mL^{-1})	Shifts in PBS (nm)	Shifts in serum (nm)	Recovery (%)
None	2.5	4.5	5.3	117.8
None	5.0	6.7	7.4	110.4
None	10.0	10.1	10.6	105.0

Credit author statement

Haohua Yang: participation and design in the whole work; drafting of the article; Formal analysis. **Xueqi Zhao**: participation in part of the work. **Ziwei Zhang**: guidance in part of the experiment. **Pinyi Ma**: guidance in the revision of experimental manuscripts. **Xinghua Wang**: guidance in the revision of experimental manuscripts. **Daqian Song**: guidance and final approval of the version to be published. **Ying Sun**: guidance and final approval of the version to be published.

Declaration of competing interest

The authors declare that they have no known competing financial

interests or personal relationships that could have appeared to influence the work reported in this paper.

Acknowledgments

This work was supported by Science and Technology Developing Foundation of Jilin Province of China (No. 20200404173YY).

Appendix A. Supplementary data

Supplementary data to this article can be found online at https://doi.org/10.1016/j.talanta.2022.123496.

References

[1] P. Nancy, J. Jose, N. Joy, S. Valluvadasan, R. Philip, R. Antoine, S. Thomas, N. Kalarikkal, Fabrication of silver-decorated graphene oxide nanohybrids via pulsed laser ablation with excellent antimicrobial and optical limiting performance, Nanomaterials 11 (4) (2021) 880, https://doi.org/10.3390/nano11040880.

[2] Q. Zhao, Q. Wu, P. Ma, L. Xu, F. Zhang, D. Li, X. Liu, S. Xu, Y. Sun, D. Song, X. Wang, Selective and sensitive fluorescence detection method for pig IgG based on competitive immunosensing strategy and magnetic bioseparation, Talanta 195 (2019) 103–108, https://doi.org/10.1016/j.talanta.2018.11.041.

[3] I. Mullor Ruiz, G. Vilarino-Feltrer, H. Mnatsakanyan, A. Valles-Lluch, M. Monleon Pradas, Development and evaluation of hyaluronan nanocomposite conduits for neural tissue regeneration, J. Biomater. Sci. Polym. Ed. 32 (17) (2021) 2227–2245, https://doi.org/10.1080/09205063.2021.1963930.

[4] J.Y. Yu, W. Niedenthal, B.M. Smarsly, M.M. Natile, Y.X. Huang, M. Carraro, Au nanoparticles supported on piranha etched halloysite nanotubes for highly efficient heterogeneous catalysis, Appl. Surf. Sci. 546 (2021) 149100, https://doi.org/10.1016/j.apsusc.2021.149100.

[5] S. Liang, W. Chen, S. Yin, S.J. Schaper, R. Guo, J. Drewes, N. Carstens, T. Strunskus, M. Gensch, M. Schwartzkopf, F. Faupel, S.V. Roth, Y.-J. Cheng, P. Mueller-Buschbaum, Tailoring the optical properties of sputter-deposited gold nanostructures on nanostructured titanium dioxide templates based on in situ grazing-incidence small-angle X-ray scattering determined growth laws, ACS Appl. Mater. Interfaces 13 (12) (2021) 14283–14295, https://doi.org/10.1021/acsami.1c00972.

[6] E. Constantin, P. Varasteanu, I. Mihalache, G. Craciun, R.-A. Mitran, M. Popescu, A. Boldeiu, M. Simion, SPR detection of protein enhanced by seedless synthesized gold nanorods, Biophys. Chem. 279 (2021) 106691, https://doi.org/10.1016/j.bpc.2021.106691.

[7] S. Al-Ariki, N.A.A. Yahya, S.a.A. Al-A'nsi, M.H.H. Jumali, A.N. Jannah, R. Abd-Shukor, Synthesis and comparative study on the structural and optical properties of ZnO doped with Ni and Ag nanopowders fabricated by sol gel technique, Sci. Rep. 11 (1) (2021) 11948, https://doi.org/10.1038/s41598-021-91439-1.

[8] R. Dobrucka, A. Romaniuk-Drapala, M. Kaczmarek, Biologically synthesized of Au/Pt/ZnO nanoparticles using Arctium lappa extract and cytotoxic activity against leukemia, Biomed. Microdevices 22 (4) (2020) 72, https://doi.org/10.1007/s10544-020-00526-z.

[9] V. Ramya, V. Kalaiselvi, S.K. Kannan, M. Shkir, H.A. Ghramh, Z. Ahmad, P. Nithiya, N. Vidhya, Facile synthesis and characterization of zinc oxide nanoparticles using psidium guajava leaf extract and their antibacterial applications, Arabian J. Sci. Eng. 47 (1) (2021) 909–918, https://doi.org/10.1007/s13369-021-05717-1.

[10] Z. Latif, M.J. Crupie, Aberrant thyroid function tests in a patient taking biotin supplements, Cureus 11 (8) (2019), e5297, https://doi.org/10.7759/cureus.5297.

[11] J.H.T. Luong, K.B. Male, J.D. Glennon, Biotin interference in immunoassays based on biotin-strept(avidin) chemistry: an emerging threat, Biotechnol. Adv. 37 (5) (2019) 634–641, https://doi.org/10.1016/j.biotechadv.2019.03.007.

[12] D. Lin, C. Mei, A. Liu, H. Jin, S. Wang, J. Wang, Cascade signal amplification for electrochemical immunosensing by integrating biobarcode probes, surface-initiated enzymatic polymerization and silver nanoparticle deposition, Biosens. Bioelectron. 66 (2015) 177–183, https://doi.org/10.1016/j.bios.2014.10.074.

[13] M. Ozawa, T. Ozawa, M. Nishio, K. Ueda, The role of CH/pi interactions in the high affinity binding of streptavidin and biotin, J. Mol. Graph. Model. 75 (2017) 117–124, https://doi.org/10.1016/j.jmgm.2017.05.002.

[14] X. Ding, Y. Yan, S. Li, Y. Zhang, W. Cheng, Q. Cheng, S. Ding, Surface plasmon resonance biosensor for highly sensitive detection of microRNA based on DNA super-sandwich assemblies and streptavidin signal amplification, Anal. Chim. Acta 874 (2015) 59–65, https://doi.org/10.1016/j.aca.2015.03.021.

[15] Q. Zhai, Y. He, X. Li, J. Guo, S. Li, G. Yi, A simple and ultrasensitive electrochemical biosensor for detection of microRNA based on hybridization chain reaction amplification, J. Electroanal. Chem. 758 (2015) 20–25, https://doi.org/10.1016/j.jelechem.2015.10.010.

[16] X. Yue, J. Sun, T. Yang, Q. Dong, T. Li, S. Ding, X. Liang, K. Feng, X. Gao, M. Yang, G. Huang, J. Zhang, Rapid detection of Salmonella in milk by a nuclear magnetic resonance biosensor based on the streptavidin-biotin system and O-carboxymethyl chitosan target gadolinium probe, J. Dairy Sci. 104 (11) (2021) 11486–11498, https://doi.org/10.3168/jds.2021-20716.

[17] Q. Qu, J. Wang, C. Zeng, M. Wang, W. Qi, Z. He, AuNP array coated substrate for sensitive and homogeneous SERS-immunoassay detection of human immunoglobulin G, RSC Adv. 11 (37) (2021) 22744–22750, https://doi.org/10.1039/d1ra02404c.

[18] A. Dosanjh, Chronic pediatric pulmonary disease and primary humoral antibody based immune disease, Respir. Med. 105 (4) (2011) 511–514, https://doi.org/10.1016/j.rmed.2010.11.013.

[19] N.I. Nii-Trebi, Emerging and neglected infectious diseases: insights, advances, and challenges, BioMed Res. Int. (2017) 5245021, https://doi.org/10.1155/2017/5245021, 2017.

[20] Y. Yu, J.E. Fisher, J.B. Lillegard, B. Rodysill, B. Amiot, S.L. Nyberg, Cell therapies for liver diseases, Liver Transplant. 18 (1) (2012) 9–21, https://doi.org/10.1002/lt.22467.

[21] E. Myasoedova, New era for outcomes and management of rheumatoid arthritis: facing the individualized treatment challenge, Joint Bone Spine 88 (3) (2021) 105066, https://doi.org/10.1016/j.jbspin.2020.08.001.

[22] C. Zong, F. Jiang, X. Wang, P. Li, L. Xu, H. Yang, Imaging sensor array coupled with dual-signal amplification strategy for ultrasensitive chemiluminescence immunoassay of multiple mycotoxins, Biosens. Bioelectron. 177 (2021) 112998, https://doi.org/10.1016/j.bios.2021.112998.

[23] Y.F. He, J.W. Chen, C.Z. An, X.L. Hou, Z.T. Zhong, C.Q. Li, W. Chen, B. Liu, Y. D. Zhao, Labeling of liver cells with CdSe/ZnS quantum dot-based fluorescence probe below freezing point, Spectrochim. Acta Mol. Biomol. Spectrosc. 263 (2021) 120203, https://doi.org/10.1016/j.saa.2021.120203.

[24] B.P. Dasanayaka, J. Zhao, J. Zhang, Y. Huang, M.U. Khan, H. Lin, Z. Li, Development of a sensitive sandwich-ELISA assay for reliable detection of fish residues in foods, Anal. Biochem. 635 (2021) 114448, https://doi.org/10.1016/j.ab.2021.114448.

[25] X.-m. Liu, X.-l. Wang, Z.-f. Qiu, Y.-d. Wang, B. Zhang, C. Xu, H.-z. Yin, Surface plasmon resonance sensing technology is applied to small molecule detection, Spectrosc. Spectr. Anal. 41 (2) (2021) 511–516, https://doi.org/10.3964/j.issn.1000-0593(2021)02-0511-06.

[26] V. Yesudasu, H.S. Pradhan, R.J. Pandya, Recent progress in surface plasmon resonance based sensors: a comprehensive review, Heliyon 7 (3) (2021), e06321, https://doi.org/10.1016/j.heliyon.2021.e06321.

[27] M. Brown, B.J. Wiley, Bromide causes facet-selective atomic addition in gold nanorod syntheses, Chem. Mater. 32 (15) (2020) 6410–6415, https://doi.org/10.1021/acs.chemmater.0c01494.

[28] M. Mansouri, F. Fathi, R. Jalili, S. Shoeibie, S. Dastmalchi, A. Khataee, M.-R. Rashidi, SPR enhanced DNA biosensor for sensitive detection of donkey meat adulteration, Food Chem. 331 (2020) 127163, https://doi.org/10.1016/j.foodchem.2020.127163.

[29] S. Tian, X. Li, J. Jiang, L. Tang, H. Zhang, Y. Yu, Z. Zhang, Highly sensitive detection of rabbit IgG by electron spin resonance using CuS nanoparticles as probe, Sensor. Actuator. B Chem. 338 (2021) 129835, https://doi.org/10.1016/j.snb.2021.129835.

[30] G.Y. Shan, M.Y. Zhong, S. Wang, Y.J. Li, Y.C. Liu, The synthesis and optical properties of the heterostructured ZnO/Au nanocomposites, J. Colloid Interface Sci. 326 (2) (2008) 392–395, https://doi.org/10.1016/j.jcis.2008.06.027.

[31] L.M. Moreau, M.R. Jones, E.W. Roth, J. Wu, S. Kewalramani, M.N. O'Brien, B. R. Chen, C.A. Mirkin, M.J. Bedzyk, The role of trace Ag in the synthesis of Au nanorods, Nanoscale 11 (24) (2019) 11744–11754, https://doi.org/10.1039/c9nr03246k.

[32] M.L.B. Figueiredo, C.S. Martin, L.N. Furini, R.J.G. Rubira, A. Batagin-Neto, P. Alessio, C.J.L. Constantino, Surface-enhanced Raman scattering for dopamine in Ag colloid: adsorption mechanism and detection in the presence of interfering species, Appl. Surf. Sci. 522 (2020) 146466, https://doi.org/10.1016/j.apsusc.2020.146466.

[33] T.-Y. Kuo, Y.-C. Chung, Surface-initiated polymerization of mussel-inspired dopamine for hydrophilic coatings, Mater. Adv. 2 (17) (2021) 5686–5690, https://doi.org/10.1039/d0ma00908c.

[34] S. Li, Q. Wu, P. Ma, Y. Zhang, D. Song, X. Wang, Y. Sun, A sensitive SPR biosensor based on hollow gold nanospheres and improved sandwich assay with PDA-Ag@Fe3O4/rGO, Talanta 180 (2018) 156–161, https://doi.org/10.1016/j.talanta.2017.12.051.

[35] F. Chen, Q. Wu, D. Song, X. Wang, P. Ma, Y. Sun, Fe3O4@PDA immune probe-based signal amplification in surface plasmon resonance (SPR) biosensing of human cardiac troponin I, Colloids Surf. B Biointerfaces 177 (2019) 105–111, https://doi.org/10.1016/j.colsurfb.2019.01.053.

[36] M. Chang, Q. Wang, X. Liu, X. Shi, G. Xu, Facile synthesis of antibody-coupled polydopamine-coated magnetic graphene oxide composites for efficient immunopurification and metabolomics analysis of mitochondria, Anal. Chem. 93 (32) (2021) 11099–11107, https://doi.org/10.1021/acs.analchem.1c01101.

[37] Y.-x. Yang, X.-x. Zhao, Y. Zhang, Proteomic analysis of mammary tissues from healthy cows and clinical mastitic cows for identification of disease-related proteins, Vet. Res. Commun. 33 (4) (2009) 295–303, https://doi.org/10.1007/s11259-008-9177-0.

[38] H. Zhang, D. Song, S. Gao, H. Zhang, J. Zhang, Y. Sun, Enhanced wavelength modulation SPR biosensor based on gold nanorods for immunoglobulin detection, Talanta 115 (2013) 857–862, https://doi.org/10.1016/j.talanta.2013.06.059.

[39] H. Zhang, Y. Sun, S. Gao, H. Zhang, J. Zhang, Y. Bai, D. Song, Studies of gold nanorod-iron oxide nanohybrids for immunoassay based on SPR biosensor, Talanta 125 (2014) 29–35, https://doi.org/10.1016/j.talanta.2014.02.036.

[40] Q. Wu, D. Song, D. Zhang, Y. Sun, An enhanced SPR immunosensing platform for human IgG based on the use of silver nanocubes and carboxy-functionalized graphene oxide, Microchim. Acta 183 (7) (2016) 2177–2184, https://doi.org/10.1007/s00604-016-1853-0.

[41] K. Lee, K.C. Gupta, S.Y. Park, I.K. Kang, Anti-IgG-anchored liquid crystal microdroplets for label free detection of IgG, J. Mater. Chem. B 4 (4) (2016) 704–715, https://doi.org/10.1039/c5tb02131f.

[42] T. Minamiki, T. Minami, R. Kurita, O. Niwa, S.I. Wakida, K. Fukuda, D. Kumaki, S. Tokito, A label-free immunosensor for IgG based on an extended-gate type organic field effect transistor, Materials 7 (9) (2014) 6843–6852, https://doi.org/10.3390/ma7096843.

[43] S. Shi, L. Wang, R. Su, B. Liu, R. Huang, W. Qi, Z. He, A polydopamine-modified optical fiber SPR biosensor using electroless-plated gold films for immunoassays, Biosens. Bioelectron. 74 (2015) 454–460, https://doi.org/10.1016/j.bios.2015.06.080.

[44] Q. Wu, D. Song, D. Zhang, H. Zhang, Y. Ding, Y. Yu, Y. Sun, A highly sensitive SPR biosensor based on a graphene oxide sheet modified with gold bipyramids, and its application to an immunoassay for rabbit IgG, Microchim. Acta 182 (9-10) (2015) 1739–1746, https://doi.org/10.1007/s00604-015-1497-5.